

# Zeptogram-Scale Nanomechanical Mass Sensing

Y. T. Yang,<sup>†</sup> C. Callegari,<sup>‡</sup> X. L. Feng, K. L. Ekinci,<sup>§</sup> and M. L. Roukes\*

Kavli Nanoscience Institute, California Institute of Technology, Mail Code 114-36,  
Pasadena, California 91125

Received October 29, 2005; Revised Manuscript Received February 5, 2006

## ABSTRACT

Very high frequency (VHF) nanoelectromechanical systems (NEMS) provide unprecedented sensitivity for inertial mass sensing. We demonstrate *in situ* measurements in *real time* with mass noise floor  $\sim 20$  zg. Our best mass resolution corresponds to  $\sim 7$  zg, equivalent to  $\sim 30$  xenon atoms or the mass of an individual 4 kDa molecule. Detailed analysis of the ultimate sensitivity of such devices based on these experimental results indicates that NEMS can ultimately provide inertial mass sensing of individual intact, electrically neutral macromolecules with single-Dalton (1 amu) resolution.

Electromechanical devices, especially those at the nanoscale, offer new prospects for a variety of important applications ranging from electronic communications to fundamental science.<sup>1</sup> In particular, electromechanical sensors are ubiquitous, having a long history of important applications in many diverse fields of science and technology. Among the most responsive are sensors based on the acoustic vibratory modes of crystals,<sup>2,3</sup> thin films,<sup>4</sup> and, more recently, microelectromechanical systems (MEMS)<sup>5,6</sup> and nanoelectromechanical systems (NEMS).<sup>7,8</sup> Two attributes of NEMS devices—minuscule mass and high quality factor ( $Q$ )—provide them with unprecedented potential for mass sensing, demonstrated by recently achieved femtogram<sup>7</sup> and attogram resolution.<sup>8</sup> Attainment of zeptogram (1 zg =  $10^{-21}$  g) resolution shown herein opens many new possibilities; among them is directly “weighing” the inertial mass of individual, electrically neutral macromolecules.<sup>9</sup> Such sensitivity also enables the observation of extremely minute (statistical) mass fluctuations that arise from the adsorption and desorption of atomic species upon the surfaces of NEMS devices—processes that impose fundamental sensitivity limits upon nanoscale gas sensors.<sup>10–12</sup> As an initial step toward these applications, we perform mass sensing experiments with gaseous species adsorbed on the NEMS surfaces at the zeptogram scale.

All the experiments are done *in situ* within a cryogenically cooled, ultrahigh vacuum apparatus with base pressure below

$10^{-10}$  Torr. As shown in Figure 1a, a minute, calibrated, highly controlled flux of Xe atoms or N<sub>2</sub> molecules is delivered to the device surface by a mechanically shuttered gas nozzle within the apparatus.<sup>13</sup> The nozzle has an orifice with a 100  $\mu$ m diameter aperture, which is maintained at  $T \sim 200$  K by heating it with  $\sim 1$  W of power to prevent condensation of the gas within the orifice and its supply line. Gas is delivered to this nozzle from a buffering chamber (volume  $V_C = 100$  cm<sup>3</sup> for the N<sub>2</sub> experiments, and 126 cm<sup>3</sup> for the Xe experiments), in turn maintained at temperature  $T_C = 300$  K. Prior to the commencement of a run, this chamber is pressurized with the species to be delivered and then sealed to allow escape only through the nozzle. Thereafter, the rate of pressure decrease,  $\partial P_C/\partial t$ , which is continuously monitored, is proportional to the total adsorbate delivery rate from the gas nozzle to the NEMS sensor, i.e., the number of incident atoms or molecules per unit time. The total number flux of gas atoms or molecules out of the nozzle in steady state is given by  $\partial N_C/\partial t = V_C(\partial P_C/\partial t)/(k_B T_C)$ .

As shown in Figure 1b, *real time* mass sensing is enabled by the incorporation of the NEMS device into a low-noise frequency-modulated phase-locked loop (FM-PLL) circuit designed to lock onto, and to track, the minute mechanical resonance signal embedded in large electrical background. This circuitry and its operation are described in detail elsewhere.<sup>14</sup> Briefly, as shown in Figure 1b the FM-PLL is implemented using a radio-frequency (RF) carrier at the resonant frequency of the device, which is frequency modulated, mixed-down, and subsequently demodulated using lock-in detection of a homodyne phase-locked loop.<sup>8</sup> Roughly speaking, this process generates a *quasi*-dc voltage proportional to the derivative of the resonant response with respect to frequency. As a result, the constant part of the

\* Corresponding author. Phone: +1-(626) 395-2916. Electronic mail: roukes@caltech.edu.

<sup>†</sup> Present address: AKT America, Inc., 3101 Scott Blvd., M/S 9106 P.O. Box 58039, Santa Clara, CA 95054.

<sup>‡</sup> Present address: Institute of Experimental Physics, Graz University of Technology, Petersgasse 16, A-8010 Graz, Austria/EU.

<sup>§</sup> Present address: Aerospace & Mechanical Engineering Department, Boston University, Boston, MA 02215.

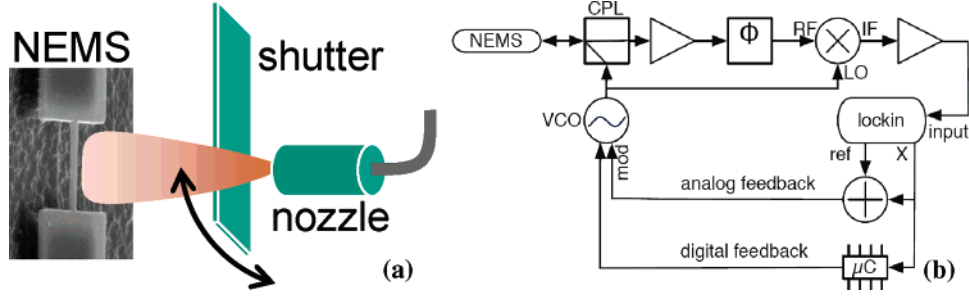


**Figure 1.** (a) Experimental configuration. A gas nozzle with a  $100\ \mu\text{m}$  aperture provides a controlled flux of atoms or molecules. The flux is gated by a mechanical shutter to provide calibrated, pulsed mass accretions upon the NEMS device. The mass flux is determined by direct measurements of the gas flow rate, in conjunction with effusive-source formulas for the molecular beam emanating from the nozzle. (b) Frequency-modulated phase-locked loop (FM-PLL) scheme. The mechanical resonance is detected in a reflection scheme, by using a directional coupler (CPL). The reflected signal is amplified, phase-shifted ( $\Phi$ ), and mixed down ( $\otimes$ ). We modulate the carrier at 1.2652 kHz and employ a lock-in amplifier (Stanford Research Systems SR830) for demodulation. The resulting output ( $\times$ ) provides the analog feedback to the VCO (Hewlett-Packard HP8648B). A computer-controlled parallel digital feedback ( $\mu\text{C}$ ) is implemented for applications requiring a large locking range.

response, which results from the ubiquitous electrical background in which the electromechanical resonance of the NEMS is embedded, is nulled out. In our experimental setup, the carrier is frequency modulated at 1.2652 kHz by the reference oscillator of a lock-in amplifier (Stanford Research Systems SR830). The mechanical resonance is detected by magnetomotive detection via a reflection bridge; the signal is coupled in and out of the device by a directional coupler. The modulated signal from the NEMS device is subsequently amplified by a low-noise amplifier, phase-shifted, and mixed down to an intermediate frequency (the modulation frequency). The lock-in is employed to detect the signal amplitude at this latter frequency. To close the analog feedback loop, the output of the lock-in amplifier is fed as a control voltage to the voltage-controlled oscillator (VCO) (Hewlett-Packard HP8648B). This imposes a proportional control with a frequency cutoff proportional to the inverse time constant of the lock-in. In addition, a digital feedback loop is established through a computer interface, which periodically checks the (digital) output of the lock-in amplifier, computes a correction, and resets the center frequency of the VCO accordingly. Effectively one has a discrete integral control, extending the locking range beyond the natural width of the resonance. We use it to follow the frequency shift induced by large changes in device mass over extended measurement intervals.

With this measurement scheme, data are obtained from two different NEMS resonators operating in their fundamental out-of-plane flexural mode: a first device (hereafter, **D133**) with fundamental resonant frequency  $f_0 = 133\ \text{MHz}$  and dimensions,  $2.3\ \mu\text{m}$  ( $l$ )  $\times$   $150\ \text{nm}$  ( $w$ )  $\times$   $70\ \text{nm}$  ( $t$ ), and a second (hereafter **D190**) with fundamental resonant frequency  $f_0 = 190\ \text{MHz}$  and dimensions,  $2.3\ \mu\text{m}$  ( $l$ )  $\times$   $150\ \text{nm}$  ( $w$ )  $\times$   $100\ \text{nm}$  ( $t$ ). Both devices are doubly clamped beams patterned from SiC epilayers,<sup>15</sup> with a quality factor of  $Q \sim 5000$  in the temperature range of the present measurements.

For the experiments described below, the NEMS devices are maintained at high vacuum ( $<10^{-7}$  Torr) at  $T = 300\ \text{K}$  for more than 1 day prior to our mass accretion studies. Subsequently, the experiments are carried out immediately

after cryogenically cooling the devices. The mass deposition rate is given by

$$\partial M_D / \partial t = m (\partial N_D / \partial t) = m A_D (\partial N_C / \partial t) / \pi L^2 \quad (1)$$

where  $m$  is the mass of adsorbed species ( $m_{\text{Xe}} = 131\ \text{amu}$ ,  $m_{\text{N}_2} = 28\ \text{amu}$ ),  $\partial N_D / \partial t$  and  $\partial N_C / \partial t$  are the number deposition rate and the total number flux from the nozzle, respectively, the factor,  $A_D / L^2$ , is the solid angle of capture subtended by the surface area,  $A_D$ , of the device exposed to the flux, and  $L$  is the distance between the device and nozzle orifice. We assume the arriving species adsorb with unity sticking probability; for our operating temperatures and choices of Xe and N<sub>2</sub>, this is a reasonable assumption.<sup>16</sup> The weighting factor  $1/\pi$  accounts for the cosine-distributed beam profile. For the N<sub>2</sub> deposition on **D190**,  $\partial N_C / \partial t = 2.25 \times 10^{12}$  molecules/s,  $L = 2.37\ \text{cm}$ , and  $A_D = 3.45 \times 10^{-13}\ \text{m}^2$ , yielding  $\partial M_D / \partial t = 20.5\ \text{zg/s}$ . For the Xe deposition experiments on **D133**,  $\partial N_C / \partial t = 2.81 \times 10^{12}$  atoms/s,  $L = 1.86\ \text{cm}$ , and  $A_D = 3.45 \times 10^{-13}\ \text{m}^2$ , these values yield  $\partial M_D / \partial t = 195\ \text{zg/s}$ .

We first demonstrate the *real time, in situ*, zeptogram-scale mass accretion upon **D190**, resulting from pulsed delivery of N<sub>2</sub> molecules at  $T = 37\ \text{K}$ , as shown in Figure 2. With a mass deposition rate  $\partial M_D / \partial t = 20.5\ \text{zg/s}$ , sequential openings of the shutter for 5 s intervals provide a series of 100 zg accretions. The resulting discretely stepped frequency shifts tracked by the FM-PLL confirm sequential, regular steps of mass accretion (each  $\sim 100\ \text{zg}$ , i.e.,  $\sim 2000\ \text{N}_2$  molecules).<sup>17</sup> The mass resolution  $\delta M$  is set by the standard deviation of frequency fluctuations on the plateaus

$$\delta M = \delta f / |\mathcal{R}| = \langle (f - f_0)^2 \rangle^{1/2} / |\mathcal{R}| \quad (2)$$

Here  $|\mathcal{R}| = |\partial f_0 / \partial M_{\text{eff}}|$  is the mass responsivity of the device;  $M_{\text{eff}}$  and  $f_0$  are the effective vibratory mass and resonant frequency of the device, respectively. The data of Figure 2 demonstrate  $\delta M \sim 20\ \text{zg}$  for the 1 s averaging time employed.

The mass responsivities for the devices are directly determined from such pulsed atom or molecule deposition

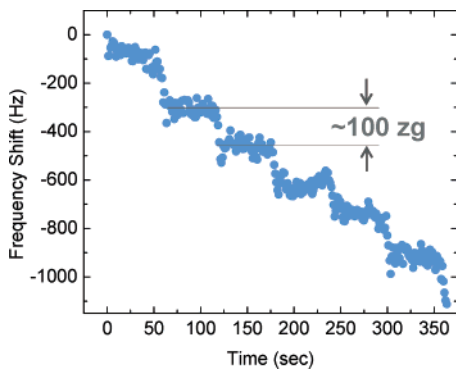


**Figure 2.** Real time zeptogram-scale mass sensing experiment. Sequential mass depositions are executed *in situ* upon the 190 MHz device within a cryogenic ultrahigh vacuum apparatus. The resulting frequency shift of the NEMS device is tracked in *real time* by a very high frequency (VHF) phase-locked loop. Each step in the data corresponds to a  $\sim 100$  zg mass accretion ( $\sim 2000$   $N_2$  molecules) resulting from opening the mechanical shutter for 5 s. The root mean square frequency fluctuations of the system correspond to a mass resolution  $\delta M \sim 20$  zg for the 1 s averaging time employed.

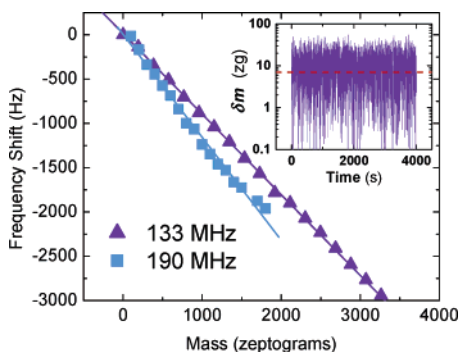


**Figure 3.** Mass responsivities of nanomechanical devices. The mass responsivities (resonant frequency shifts versus accreted mass) are measured for two VHF NEMS devices (operating at 133 and 190 MHz). Xe atoms are accreted at  $T = 46$  K upon the 133 MHz device with  $\sim 200$  zg mass increments per data point (purple).  $N_2$  molecules are accreted at  $T = 37$  K upon the 190 MHz device with  $\sim 100$  zg mass increments per data point (blue). The slopes of the mass loading curves directly exhibit the unprecedented mass responsivity of the order of 1 Hz/zg. (right inset) Mass resolution. The “mass noise floor” for the 133 MHz device, which originates from its frequency-fluctuation noise, is measured with 1 s averaging time over the course of  $\sim 4000$  s while it is temperature-stabilized at 4.2 K with zero applied gas flux. The average root mean square value (red dashed line), reflects attainment of  $\sim 7$  zg (i.e.,  $\sim 4$  kDa) mass resolution, the equivalent of  $\sim 30$  Xe atoms.

measurements. Data are shown both for **D190** (for conditions described above) and for **D133** in Figure 3. We expose **D133** to Xe with mass deposition rate  $\partial M_D/\partial t = 195$  zg/s and opening shutter for 1 s yields  $\sim 200$  zg mass accretion per data point (each  $\sim 900$  Xe atoms) at  $T = 46$  K. Both devices demonstrate unprecedented responsivities:  $|\mathcal{R}|$ , directly extracted from the slope of the linear fit, at the level of roughly 1 Hz shift per zeptogram of accreted mass. More precisely, we find  $|\mathcal{R}_{D133}| \approx 0.96$  Hz/zg and  $|\mathcal{R}_{D190}| \approx 1.16$  Hz/zg. These values are in excellent agreement with the theoretical estimates from the expression  $|\mathcal{R}| \approx f_0/2M_{\text{eff}}$ ,

which yields  $\sim 0.89$  Hz/zg for **D133** ( $M_{\text{eff}} \approx 73$  fg) and  $\sim 0.99$  Hz/zg for **D190** ( $M_{\text{eff}} \approx 96$  fg).<sup>8,9</sup>

Our highest mass resolution, at present, is demonstrated with **D133** stabilized at  $T = 4.2$  K.<sup>18</sup> Exceptionally small fractional frequency fluctuations  $\delta f/f_0 = \langle (f - f_0)^2 \rangle^{1/2}/f_0 \sim 5 \times 10^{-8}$  (50 ppb) are observed over the course of a  $\sim 4000$  s interval with 1 s averaging time (right inset of Figure 3). This demonstrates attainment of a mass resolution of  $\delta M \sim 7$  zg, equivalent to accretion of  $\sim 30$  Xe atoms or, alternatively, of an *individual* 4 kDa macromolecule. Using  $M_{\text{eff}} \approx 73$  fg,  $Q \sim 5000$ , and dynamic range DR  $\sim 80$  dB, such a mass resolution is consistent with the estimated value 2.9 zg from the expression

$$\delta M \sim (M_{\text{eff}}/Q)10^{-\text{DR}/20} \quad (3)$$

as described by Ekinci et al.<sup>9</sup> Our current dynamic range is determined, at the bottom end, by the noise floor of the posttransducer readout amplifier of the NEMS device and, at the top end, by the onset of nonlinearity arising from the Duffing instability for a doubly clamped beam.<sup>19</sup> With our current experimental setup, we are able to track mass accretions up to a total of  $\sim 2.3 \times 10^6$  xenon atoms on **D190**, with no observable change in the quality factor. This confirms a remarkably large mass dynamic range from a few kilodaltons (or several zeptogram sensitivity) up to at least the  $\sim 100$  MDa range, corresponding to femtogram-scale accretions.<sup>12</sup>

In conclusion, we demonstrate NEMS mass sensing at the zeptogram scale. The agreement between predicted values for both the mass responsivity  $|\mathcal{R}|$  and mass resolution  $\delta M$  confirms our analyses and validates their use in projecting a path to single-Dalton (1 amu) mass resolution from eq 3.<sup>9</sup> Attainment of this goal is possible, for example, with a device having a fundamental resonant frequency of 1 GHz, vibratory mass  $M_{\text{eff}} \sim 1 \times 10^{-16}$  g, and  $Q \sim 10\,000$ , using a displacement readout system providing a dynamic range, DR  $\sim 80$  dB. These are quite realistic parameters for next generation NEMS—in fact, we have already demonstrated each separately. We recently demonstrated NEMS vibrating in fundamental mode at microwave frequencies.<sup>20</sup> In conjunction with our recent development of techniques for improved  $Q$ ,<sup>21</sup> and the advances in frequency-shift readout in the tens of ppb range employed in these measurements, it is clear that NEMS sensing at the level of single-Dalton will soon be attained.<sup>9</sup> Realization of NEMS mass sensors with single-Dalton resolution will make feasible the detection of *individual*, intact, electrically neutral macromolecules with masses ranging well into the tens and hundreds MDa range. This is an exciting prospect—when realized it will blur the traditional distinction between inertial mass sensing and mass spectrometry. We anticipate that it will also open intriguing possibilities in the life sciences and atomic physics.<sup>22</sup>

**Acknowledgment.** We gratefully acknowledge support from DARPA MTO under Grant DABT63-98-1-0012, from DARPA/SPAWAR under Grant N66001-02-1-8914, and from the NSF under Grant ECS-0089061.

## References

- (1) Roukes, M. L. *Phys. World* **2001**, *14*, 25.
- (2) Ballantine, D. S.; et al. *Acoustic Wave Sensors*; Academic Press: San Diego, CA, 1997.
- (3) Lu, C. *Application of Piezoelectric Quartz Crystal Microbalance*; Elsevier: London, 1984.
- (4) Thompson, M.; Stone, D. C. *Surface-Launched Acoustic Wave Sensors: Chemical Sensing and Thin Film Characterization*; John Wiley and Sons: New York, 1997.
- (5) Thundat, J.; Wachter, E. A.; Sharp, S. L.; Warmack, R. J. *Appl. Phys. Lett.* **1995**, *66*, 1695.
- (6) Davis, Z. J.; Abadal, G.; Kuhn, O.; Hansen, O.; Grey, F.; Boisen, A. *J. Vac. Sci. Technol., B* **2000**, *18*, 612.
- (7) Lavrik, N. V.; Datskos, P. G. *Appl. Phys. Lett.* **2003**, *82*, 2697.
- (8) Ekinici, K. L.; Huang, H. X. M.; Roukes, M. L. *Appl. Phys. Lett.* **2004**, *84*, 4469. Attogram-scale mass sensing is first described in *Apparatus and method for ultrasensitive nanoelectromechanical mass detection*, Roukes, M. L. and Ekinici, K. L., U.S. Patent 6,722,200 (filed May 4, 2001, awarded April 20, 2004).
- (9) Ekinici, K. L.; Yang, Y. T.; Roukes, M. L. *J. Appl. Phys.* **2004**, *95*, 2682.
- (10) Cleland, A. N.; Roukes, M. L. *J. Appl. Phys.* **2002**, *92*, 2758.
- (11) Yong, Y. K.; Vig, J. R. *IEEE Trans. Ultrason., Ferroelectr. Freq. Control* **1989**, *36*, 452.
- (12) Yang, Y. T.; Callegari, C.; Feng, X. L.; Roukes, M. L. In preparation.
- (13) Pauly, H. in *Atomic and Molecular Beam Methods*; Scoles, G., Ed.; Oxford University Press: New York, 1988.
- (14) Callegari, C.; Yang, Y. T.; Feng, X. L.; Roukes, M. L. In preparation.
- (15) Yang, Y. T.; et al. *Appl. Phys. Lett.* **2001**, *78*, 162.
- (16) Kreuzer, H. J.; Gortel, Z. W. *Physisorption Kinetics*; Springer-Verlag: Berlin, 1986. At low coverage, unity sticking probabilities are observed for Xe on W(100) at  $T = 65$  K, Xe on Ni(100) at  $T = 30$  K, and N<sub>2</sub> on Ni(110)  $T = 87$  K. We expect the above to be representative materials and conditions, so that the cryogenic adsorption upon the NEMS device will behave similarly in our case.
- (17) We confirm that there is negligible thermal perturbation to the NEMS response from adsorbing species.
- (18) Note that deposition experiments could not be performed at this temperature, because of the conflicting requirements of keeping the nozzle warm while keeping the device as cold as possible. This is only a limitation of our present setup and is not a general one.
- (19) Postma, H. W. C.; Kozinsky, I.; Husain, A.; Roukes, M. L. *Appl. Phys. Lett.* **2005**, *86*, 223105.
- (20) Huang, X. M. H.; Zorman, C. A.; Mehregany, M.; Roukes, M. L. *Nature* **2003**, *421*, 496.
- (21) Huang, X. M. H.; Feng, X. L.; Zorman, C. A.; Mehregany, M.; Roukes, M. L. *New J. Phys.* **2005**, *7*, 247.
- (22) Hänsel, W.; Hommelhoff, P.; Hänsch, T. W.; Reichel, J. *Nature* **2001**, *413*, 498.

NL052134M